Validation of EXAFS Analysis of Iridium Compounds

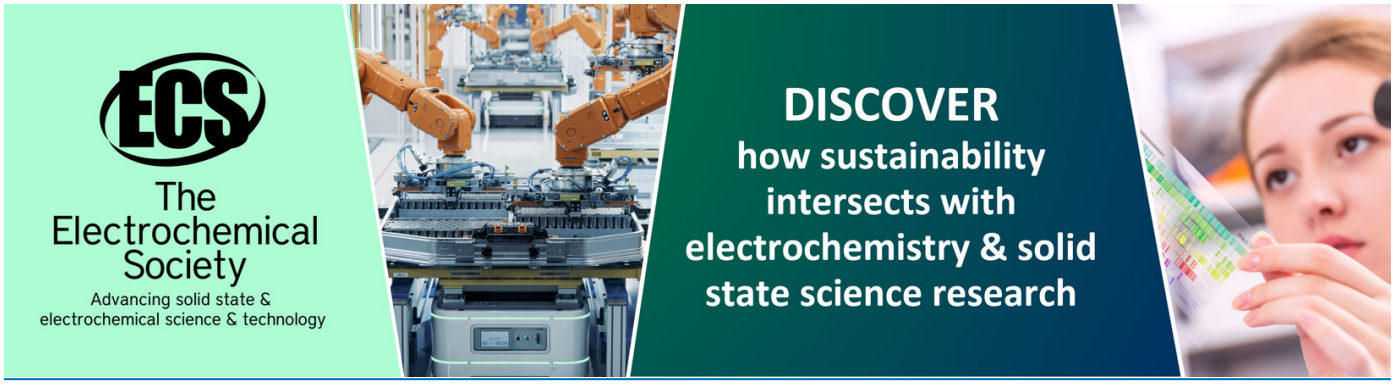

Journal of Physics: Conference Series **712** (2016) 012059 doi:10.1088/1742-6596/712/1/012059

Validation of EXAFS Analysis of Iridium Compounds

M. C. Feiters,[1] A. Longo,[2] D. Banerjee,[2] C. J. M. van der Ham,[3] D. G. H. Hetterscheid[3]

[1] Institute of Molecules and Materials, Radboud University, Heyendaalseweg 135, 6525 AJ Nijmegen, The Netherlands
[2] Dutch-Belgian Beamline (DUBBLE), ESRF – The European Synchrotron, CS40220, 38043 Grenoble Cedex 9, France
[3] Leiden Institute of Chemistry, Leiden University, P.O. Box 9502, 2300 RA Leiden, The Netherlands

m.feiters@science.ru.nl

Abstract. Results of iridium L_3 edge EXAFS measurements of compounds relevant for water oxidation catalysis are compared to those of other structural techniques. The structural results from EXAFS for the Ir compounds investigated here compare well to those of other structural techniques. Multiple scattering contributions are important in the coordinated Cp* and NHC ligands as well as in the $IrCl_6$ unit and the IrO_2 rutile structure. NHC is relatively weak compared to Ir, Cl, and even Cp* and O, and often out of phase with the other contributions.

1. Introduction

New water oxidation catalysts that show higher rates of conversion at milder conditions are important in the search for alternatives for fossil fuels [1], in which solar energy is stored as an energy dense chemical fuel, in a process producing oxygen from water along with a reduced fuel such as hydrogen, methane, methanol, or another hydrocarbon. [IrCp*$(OH)_2$(Me_2-NHC)] (**2**, prepared from the bis-Cl analogue **1**; Me_2-NHC = *N*-dimethylimidazolin-2-ylidene, Cp* = pentamethylcyclopentadienyl, see Fig. 1 (right) for structures) is a catalyst for water oxidation at an electrode surface [2], and parallel to the present study we investigate with EXAFS whether the iridium complex is oxidized to Ir oxide, possibly IrO_2 **3**, which is also catalytically active [3], and/or whether the Cp* and Me_2NHC ligands are still coordinated to Ir. In order to validate our approach, we describe here how we measured and simulated the EXAFS of the aforementioned Ir compounds **1-3** as well as that of the coordination compound K_2IrCl_6 **4** and the bridged dimer [{IrCp*Cl_2}$_2$] **5** (Fig. 1), of which most structures were already known by other techniques.

2. EXAFS measurements and simulations

X-ray absorption spectra were collected at the Ir L_3-edge (11215 eV) on the EXAFS station (BM26A) of the Dutch-Belgian beamline (DUBBLE) [4] at the European Synchrotron Radiation Facility (ESRF) in Grenoble, France. The Ir compounds were diluted with boron nitride and measured as pressed pellets in transmission mode at 20 K; at least 2 scans per sample were averaged to improve the signal-to-noise ratio. The EXAFS was extracted with Viper [5] and simulated with EXCURVE [6] by the same approach as in the recent study of Ir complexes with *N*-heterocyclic carbene and cyclooctadiene or pyridine ligands [7]. The geometries (distances and angles) of the carbene and cyclopentadienyl

ligands were adopted from crystallographic data for **1** [8] and **5** [9] and expressed in polar coordinates with the absorber Ir atom at the centre. Structural models (without H) were iteratively refined against the experimental data until a minimum in the fit index was reached by floating the threshold energy EF (in eV), the Debye-Waller (DW) factors (as $2\sigma^2$ in $Å^{-2}$), and the distances (R in Å) to Ir. Multiple scattering (MS) within the ligands was calculated up to 3rd order unless otherwise indicated. In order to reduce the number of parameters, the distances between the ring atoms were treated as restraints [10], so that effectively only the distance between the Ir and the ligand-donor atoms was allowed to float, while the distances between Ir and atoms in equivalent positions were averaged, and the corresponding DW factors grouped as much as possible.

3. EXAFS results

The spectra of the Ir-Cp* complexes are shown in Fig. 1. The Fourier transform (FT) of **2** (top) shows that the contributions of the atoms directly linked to Ir, 1 C atom of NHC, 5 C of the Cp* ring, and 2 O atoms, are not resolved and give a single shell at R = 2.0-2.2 Å. Compared to this, the contributions of the Me groups in the Cp* and NHC and the remote atoms of the ring of latter are relatively weak; it was expected that NHC-coordination would give a characteristic EXAFS signature similar to that observed for imidazole coordination in metalloproteins, the so-called 'camel back' [11]. Although a weak resolved feature just above 4 Å in the FT is characteristic for the NHC ring for **1** and **2**, its contribution (remotely resembling a camel back, blue trace) is hardly visible in the experimental EXAFS, in line with our earlier results for hydrogenation catalysts [7]. The Cp* contributions (black) are stronger but out of phase with that of NHC due to the slightly longer Ir-C distance.

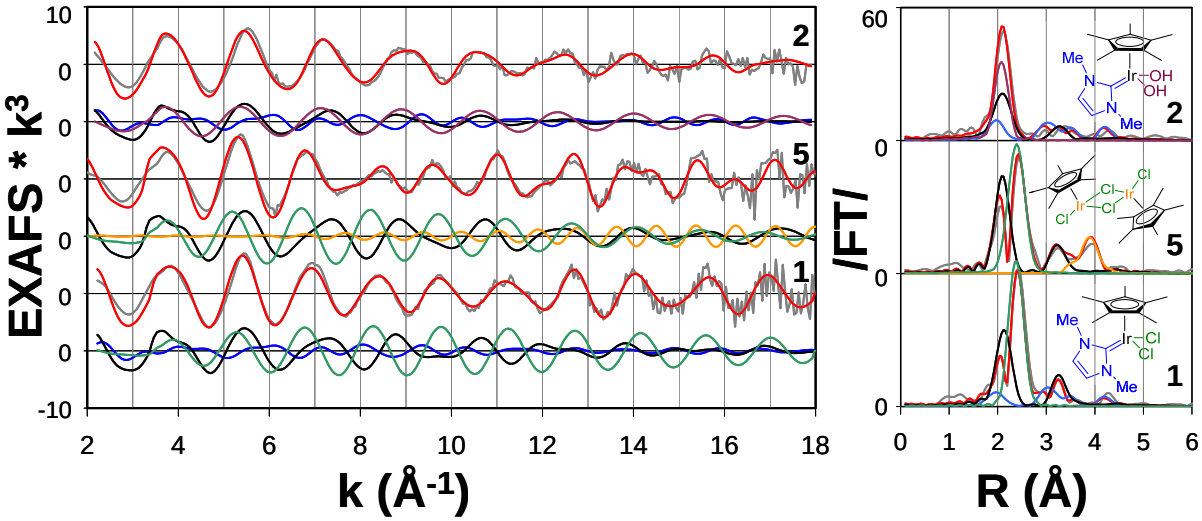

Figure 1. k^3-weighted Ir L_3 edge EXAFS (χ^*k^3, left) and phase-shifted modulus of the Fourier transform (/FT/, right) of Ir Cp* compounds **2**, **5**, and **1**. The traces below the experimental (grey) and simulated (red, see Table 1 for parameters) EXAFS and included in the FT panel represent the components: black, Cp*; blue, NHC; green, Cl; orange, Ir.

The FT of **1** (bottom) is dominated by a split major peak at 1.5-3.0 Å which contains contributions of 2 Cl backscatterers (green) at 2.4 Å, the 5 Cp-C atoms at (average) 2.2 Å, and the NHC-C atom at 2.015 Å, which are out of phase with each other for most of the range of the EXAFS. The contribution of the Cp-Me groups at 3.3 Å is relatively strong in this case, whereas that of the NHC outer ring atoms is again weak. The spectrum of **5** (middle) is similar to that of **2**, except that the contribution of NHC is replaced by one of the remote Ir at 3.77 Å, which is also evident from a strong high-frequency contribution (orange) at high k in the EXAFS. It might be expected that the 3 Cl atoms in **5** would give a stronger contribution to the EXAFS than the 2 Cl in **2**, but the crystal structure [9] detects a subtle difference between the distance from Ir to terminal (T) and bridging (B) Cl atoms (Table 1) which is

Table 1. Crystallographic and EXAFS simulation results for distances in Ir Cp* compounds

	IrCp*X_2(Me_2-NHC); **1**(X=Cl)		**2** (X=OH)	[{IrCp*Cl_2}$_2$] **5**	
	XRD (average) [8]	EXAFS [a]	EXAFS [a]	XRD ave [9]	EXAFS [a]
NHC-C	2.054	2.03(4) /.01(1)	2.03/.008	-	-
NHC-N	3.063, 3.066 (3.065)	3.08(2) /.005(4)	3.08/.005	-	-
NHC-Me	4.218, 4.251 (4.235)	4.27(4)/.01(1)	4.29/.004	-	-
NHC-C	3.526, 3.483 (3.505)	3.50(5)/.01(1)	3.50/.004	-	-
Cp-C	2.150, 2.155, 2.159, 2.228, 2.261 (2.191)	2.18(2)/.009(2)	2.16/.017	2.132	2.144(6)/.007(1)
Cp-Me	3.258, 3.310, 3.308, 3.332, 3.376 (3.319)	3.31(2)/.006(3)	3.34/.016	3.280	3.28(2)/.008(3)
OH	-	-	2.12/.003	-	-
Cl-T [b]	2.438, 2.440 (2.439)	2.426(3)/.0030(5)	-	2.387	2.37(2)/.005(2)
Cl-B [b]	-	-	-	2.453	2.45(2)/.005(1)
Ir	-	-	-	3.769	3.77(2)/.005(1)
EF (eV)	-	-11.6(6)	-11.1	-	-10.5(6)

[a] Distances in Å/Debye-Waller factors as $2\sigma^2$ in $Å^{-2}$; errors in last decimals for **1** and **5** in parentheses; [b] Cl-T, Cl-B, terminal and bridging Cl atoms respectively.

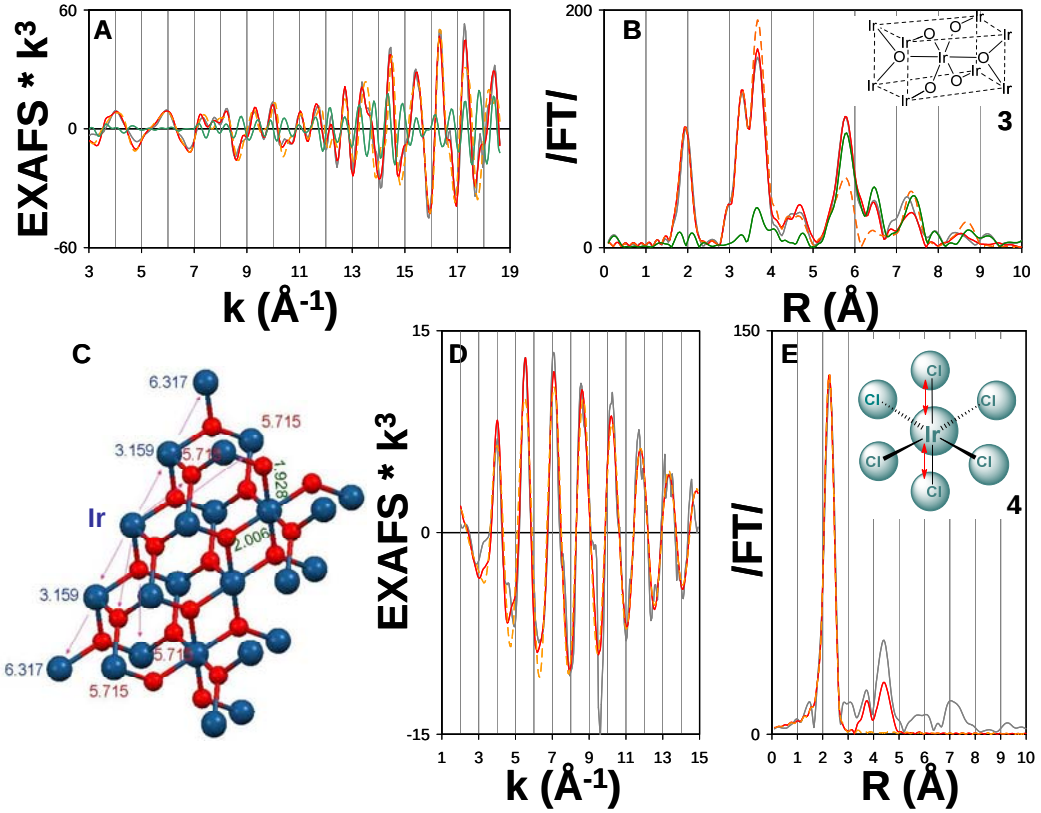

Figure 2. EXAFS (A) and FT (B, inset: schematic rutile structure) of IrO_2 **3**. (C) Quadrant of the cluster used in the simulation for **3**; central Ir labeled with 'Ir'. EXAFS (D) and FT (E, inset: $IrCl_6$ octahedron with an example of a 4th order MS pathway indicated with red arrows) of K_2IrCl_6 **4**. Traces: grey, experimental; red, best simulations; dashed orange, single scattering; green, residual MS.

detected by EXAFS as a weakening of their contribution, and adequately simulated with a split shell with same DW-factors but different distances. The good agreement (within 0.02 Å) of the distances in the refined EXAFS simulations (Table 1) with the averages of the relevant crystallographic Ir-ligand atom distances inspires confidence in the phaseshift calculations and the approach for the simulation and the refinement. The EXAFS result for **2** also agrees with that of the crystal structure of **1**, except that the Cl ligands in **1** have to be replaced by O (from OH) in **2**, which are found at 2.12 Å. The proximity of 3 unresolved shells of weak scatterers in the range 2.0-2.2 Å results however in strong correlations between the parameters and high fitting errors for **2**, which are not shown in Table 1.

The EXAFS of **3** (Fig. 2A-B) has sharp and intense features even at high k and the FT displays shells even above 10 Å (not shown). Given the many sets of atoms Ir, A, B in **3** for which the Ir-A-B angle approaches 180^{o}, the influence of MS effects on the spectrum, given in Fig. 2A-B as the difference between the complete simulation and the single scattering component (green trace) is remarkably small, as noted before [12]. In our final simulation a cluster of 126 Ir and O atoms at positions corresponding to a rutile structure (partly shown in Fig. 2C) with shells up to 8.5 Å was refined. There is a split first EXAFS shell due to a subtle tetragonal distortion of the Ir coordination geometry. The results for the nearest atoms compare well with those of neutron diffraction ([13], given in parentheses) 2 O at 1.969 (1.960); 4 O at 2.001 (1.999); 2 Ir at 3.166 (3.159); 4 O at 3.41 (3.423); 8 Ir at 3.555 (3.556-3.564) Å. Interestingly, the spectrum of **4** (Fig. 2D-E) displays an additional shell in the FT at approximately twice the distance of the expected major shell of Cl atoms at 2.32 Å. It was found that both shells could be reasonably well simulated with a unit of 6 Cl arranged in octahedral symmetry around Ir at a distance of 2.326 Å ($2\sigma^2$ = .008) and calculating the MS up to 4th order. The shell in the FT at 4.5 Å does not arise from the presence of atoms at that distance, but from a MS pathway Ir-Cl-Ir-Cl(trans)-Ir with a total path length of twice the Ir-Cl distance, indicated with red arrows in the inset in Fig. 2E. The Ir-Cl distance found corresponds reasonably well with those found in other studies for **4** (2.307 Å, [14]) and its Cs analogue (2.332 Å [15]).

4. Acknowledgements

The authors thank the Dutch and Flemish Research Councils (NWO, FWO) for the provision of beam time at the DUBBLE beamline at BM26A of the European Synchrotron Radiation Facility.

References

[1] Lewis NS, Nocera DC 2006 *Proc. Nat. Acad. Sci. U.S.A.* **103** 15279.
[2] Hetterscheid DGH, Reek JNH 2011 *Chem. Commun.* **47** 2712.
[3] Nakagawa T, Beasley CA, Murray RW 2009 *J. Phys. Chem. C* **113** 12958.
[4] Nikitenko S, Beale AM, van der Eerden AMJ, Jacques SDM, Leynaud O, O'Brien MG, Detollenaere D, Kaptein R, Weckhuysen BM, Bras W 2008 *J. Synchrotron Radiat.* **15** 632.
[5] Klementev KV 2001 *J. Phys. D Appl. Phys.* **34** 209.
[6] Gurman SJ, Binsted N, Ross I 1984 *J. Phys. C Solid State* **17** 143.
[7] van Weerdenburg BJA, Engwerda AHJ, Eshuis N, Longo A, Banerjee D, Tessari M, Fonseca Guerra C, Rutjes FPJT, Bickelhaupt FM, Feiters MC 2015 *Chem. Eur. J.* **21** 10482.
[8] Xiao XQ, Jin GX 2008 *J. Organomet. Chem.* **693** 3363.
[9] Churchill MR, Julis SA 1977 *Inorg. Chem.* **16** 1488.
[10] Binsted N, Strange RW, Hasnain SS 1992 *Biochemistry* **31** 12117.
[11] Feiters MC, Navaratnam S, Al-Hakim M, Allen JC, Spek AL, Veldink GA, Vliegenthart JFG 1988 *J. Am. Chem. Soc.* **110** 7746.
[12] Prouzet E 1995 *J. Phys.-Condens. Mat.* **7** 8027.
[13] Bolzan AA, Fong C, Kennedy BJ, Howard CJ 1997 *Acta Crystallogr. B* **53** 373.
[14] Lindop AJ 1970 *J. Phys. Part C Solid* **3** 1984.
[15] Coll RK, Fergusson JE, Penfold BR, Rankin DA, Robinson WT 1990 *Inorg. Chim. Acta* **177** 107.